NRIAG JOURNAL OF ASTRONOMY AND GEOPHYSICS
2020, VOL. 9, NO. 1, 362–374
https://doi.org/10.1080/20909977.2020.1746891

Mapping the archaeological relics of catacombs at Northeast Saqqara using GPR data, Egypt

Abdel-Monem S. Mohamed[a], Magdy Atya[a,b], Nadia AbouAly[a], Karrar El Farragawy[c], Esraa E. Hegazy[a], Mohamed Saleh[a,d], Khamis Kabeel[a] and Asmaa A. El-Mahdi[b]

[a]Geodynamic Department, National Research Institute of Astronomy and Geophysics, Cairo, Egypt; [b]Interscient Technology, Earth Imaging Systems and Consulting, Nasr City, Egypt; [c]Geology Department, Faculty of Science, Aswan University, Aswan, Egypt; [d]IPGS (UMR7516), EOST Université de Strasbourg, CNRS, Strasbourg, France

ABSTRACT

Ground Penetrating Radar "GPR" is a powerful geophysical technique capable to collect and record detailed information about the shallow earth's subsurface. Its application to map archaeological ruins is growing fast and getting more precise. GPR technique involves transmitting radar waves from a transmitting antenna, reflecting the waves off buried discontinuities and measuring the elapsed time before the reflections are received again at the surface by a receiving antenna. The area of interest is Saqqara. The data acquiring procedure and field notes could be considered as the start point to process and interpret collected data sets. They help also to bring the study's outcome in an easy form, either in 2D and/or 3D images, understandable by archaeologists. The generated images provide primary feedback that could be used to establish an excavation site or to identify significant areas containing cultural remains that would be better left untouched; therefore, the information can guide archaeologists to avoid destructing these locations. The present data set includes three grids (Grid 1, Grid 2, and Free-line Grid) in the sum of 81 measuring lines. The data were acquired using SIR4000 connected to a 200 MHz antenna applying time range of 200 ns with 1024 samples to fulfil adequate resolution in depth and 80 scans per length for appropriate resolution in scan direction. Global Navigation Satellite System (GNSS) network is constructed to improve the GPS measurements over the entire site's location and elevation. The data were processed in a way to minimise the undesired signals and to emphasise the signals of use, and it was interpreted to reveal the existence of archaeological remains. The results uncover the finding of incredible varieties of archaeological objects such as tombs, sub-tunnels and catacombs, etc. It was also noticed that depth of interest ranges from 0.6 to 3 metres on the basis of wave velocity of 0.1 m/ns.

ARTICLE HISTORY
Received 4 August 2019
Revised 17 March 2020
Accepted 19 March 2020

KEYWORDS
Saqqara area; catacombs; archaeology; GPR; data acquisition and analysis

1. Introduction

Saqqara is one of the most important archaeological sites in Egypt. It is located on the western bank of the Nile, about 15 km to the southwest of Giza and 30 km south of modern-day Cairo, and it is part of the vast Memphis Necropolis. A Numerous royal tombs dated to the Old Kingdom period (about 2600–2100 BC) are preserved in the cemetery area with a dominant step pyramid complex built in the 3rd Dynasty by Djoser-Netjerykhet about 2650 BC (Adès 2007). Beneath the sands of northern Saqqara is a wide network of catacombs, crammed with the remains of millions of mummified animals. The sampling of small areas and bone examination of their contents suggest that the entire network is home to eight million dogs, as well as a handful of cats and jackals (Lehner 1997). It is thought that a small tunnel was built to remove animal mummies which were then likely ground up and sold as fertiliser (Harry 2007). A detailed map of Saqqara area is drawn up showing all the archaeological sites and exploratory mission sites operating in Saqqara area are given in Figure 1.

Ground Penetrating Radar "GPR" is commonly used for archaeological investigations. The technique is very time effective and cost saver, i.e., it helps to reveal wide areas in short times and low cost. Its capability to map the fine details within the near-surface mediums makes it powerful to construct 3D geophysical-maps and images of the subsurface at archaeological sites. GPR technique involves transmitting radar waves from a surface antenna, reflecting them off buried discontinuities and measuring the elapsed time before the reflections are received again at the surface (Shaaban et al. 2009; Davis and Annan 1989). The development of the amplitude slice maps and computer programs made GPR technology more understandable to the archaeological community and able to produce synthetic computer models of buried archaeological features and associated stratigraphy. In Egypt, GPR is successfully used in imaging the subsurface at several archaeological sites (Khozym 2003, 2007; Hafez et al. 2008; Sayed 2012; Atya et al. 2012). In this study, the GPR survey is conducted using SIR4000 with the 200 MHz, and zig-zag configuration is

CONTACT Abdel-Monem S. Mohamed abdel_monem@yahoo.com National Research Institute of Astronomy and Geophysics, Cairo, Egypt

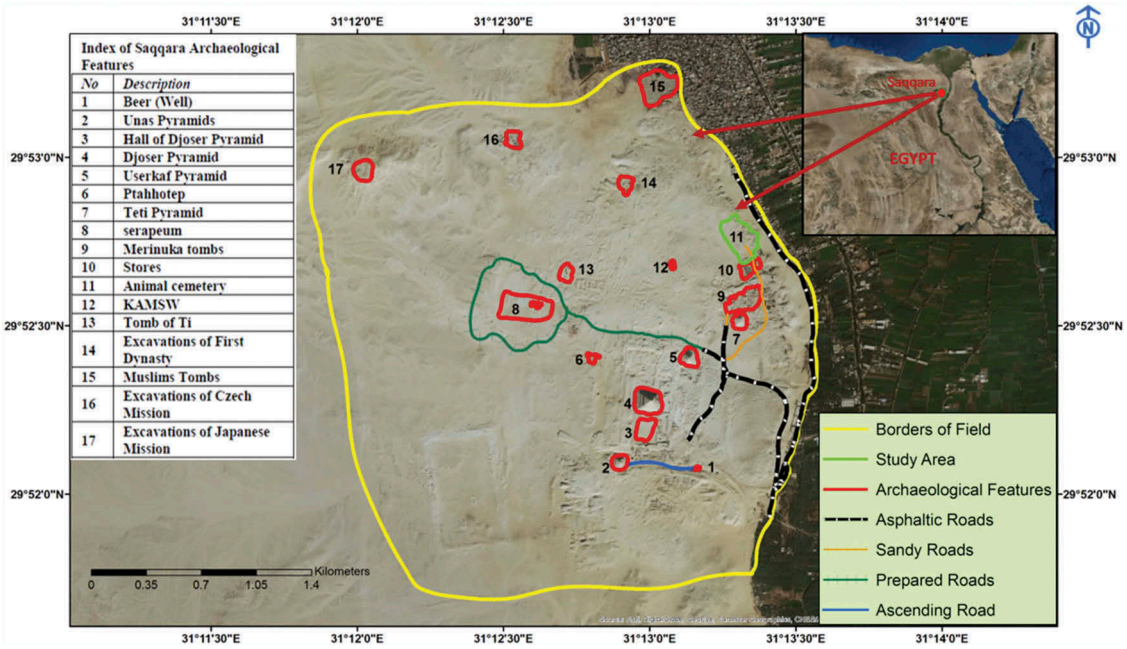

Figure 1. A detailed map is showing all the archaeological sites and exploratory mission sites operating in the Saqqara area.

implemented to acquire 3D grids at cells 1, 2 and free lines grid. The outcome is a series of 2D section and slice maps for different depths. Several signatures for corridors, catacombs and rooms of burial at shallow depths are identified and further field investigation is required. The Ground Penetrating Radar (GPR) is a non-destructive electromagnetic geophysical tool for detecting subsurface anomalies and for estimating physical characteristics of a medium in several geosciences and engineering applications (Elkarmoty et al. 2017). GPR is superior as its control units and antennae can be carried in a cart or towed by a vehicle traversing at highway speed (Lai et al. 2018). GPR is one of the most effective tools for the characterisation of ground conditions in urban areas (Hong et al. 2018).

Global Navigation Satellite System (GNSS) reference point network composed of five stations is constructed. They are left for a sufficient time to enhance the accuracy of the coordinates and elevations. Then, the entire site is surveyed using Stop-and-Go technique; the stop locations are on significant places to the GPR survey, and the collected data are corrected to the GNSS reference points.

2. Meaning of artefact to GPR concepts

GPR technique involves transmitting high frequency electromagnetic (EM) pulses from a surface sender into the ground. If EM waves strike an object, they will bounce back to the surface. The time elapsed between the pulse being sent and received back will provide evidence of depth. This process is enhanced when hundreds of reflections are measured and recorded by antennas. They are operated in a close crisscross grid scheme to create a three-dimensional interpretation of the sediment and feature changes under the surface.

All sedimentary strata and buried artefacts in the ground have physical and chemical properties that influence the velocity of the EM energy spread. Variations of the returned wave energy are indicative of underlying archaeological features. Antennas that are located above the ground will not work effectively as their energy waves will fail to penetrate the ground, as most will be reflected back from the ground surface.

3. Field survey

3.1. Topographic survey

It was necessary to elevate the topography of the area proposed for the investigation; probably it would not be possible to compensate the ground surface's topography in digital records, but gives at least a declaration for removing the evenness effects on the data. GNSS technique of surveying is selected for constructing a reference station network composed of five reference stations. Locations of such stations should be carefully picked, where the stations' locations are in a clear area, far away from any electromagnetic sources and metal structures, and mount all reference stations on a homogeneous bedrock, if possible. The reference GNSS network of five stations is established in Saqqara plateau for determining and enhancing the accuracy of the coordinates and elevations as shown in Figure 2. Then, the measurements of the GPS points along all the grids (as in Figure 3)

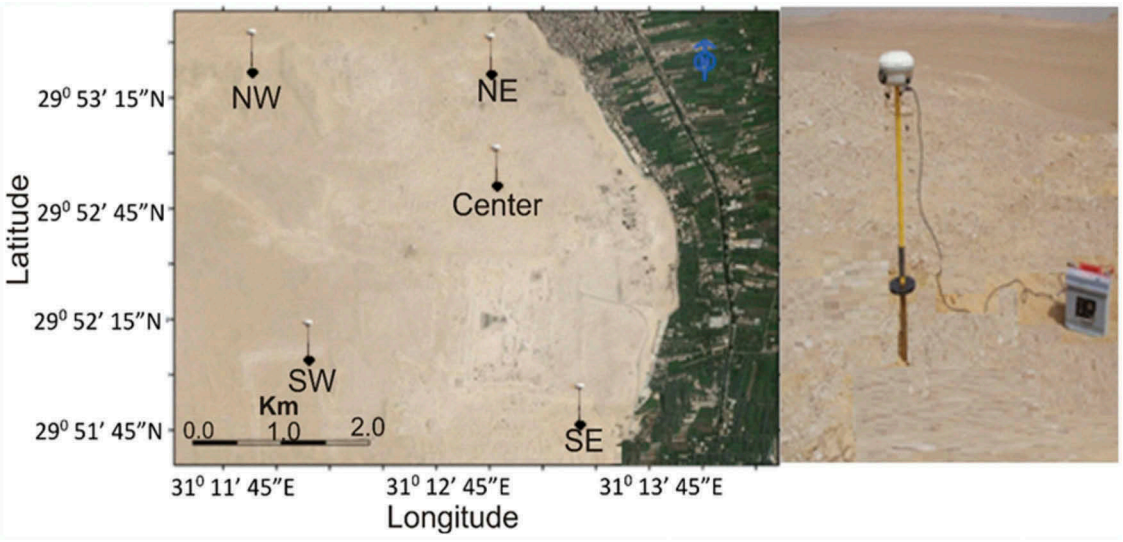

Figure 2. Construction of the GNSS reference station network in Saqqara area.

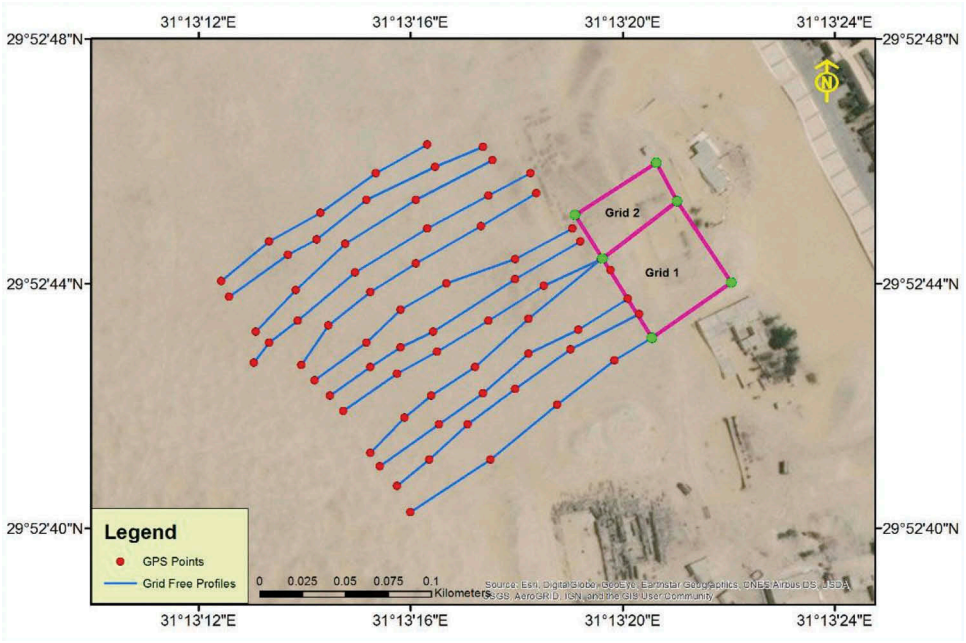

Figure 3. A map of the location GPR three grids in the survey area.

associated with GPR survey are performed using receiver's type Trimble R8 using the Stop-and-Go technique and they are corrected to the GNSS reference points. Processing of the data set is performed using Trimble Business Center software package (Trimble 2015) and other programs for the adjustment. The sampling interval and elevation mask angle are fixed throughout the survey at 1 sec and 5°, respectively. The international GNSS service (IGS) precise ephemeris is applied in the calculation. GNSS results gave a highly topographic map with accuracy within millimetre. The topographic map, resulting from the analysis, is plotted in Figure 4.

3.2. GPR data collection

The Sub-surface Interface Radar (SIR) model SIR4000 System (form the Geophysical Survey System Incorporation (GSSI)) is used to collect the data at the site. It is connected to a 200 MHz antenna and a survey wheel as shown in Figure 5. Eighty-one GPR profiles were carried out in zig-zag pattern distributed on three grids; 1, 2, and Free-Line (as in Figure 3). The first grid (Grid 1: 50 m x 50 m) includes 34 GPR profiles, the second grid (Grid2: 50 m x 25 m) includes 35 GPR profiles, and the free-line grid includes 12 GPR profiles with different lengths.

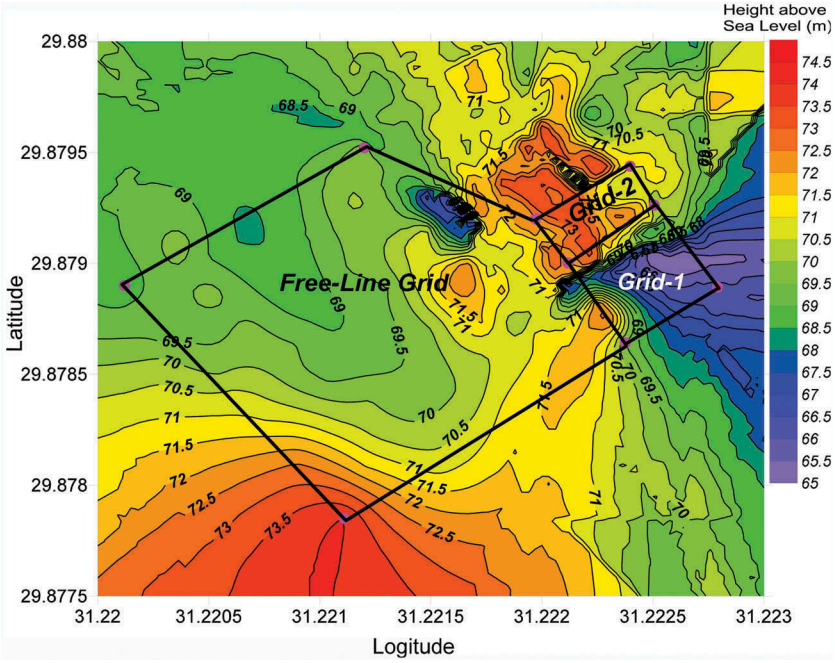

Figure 4. Topographic map of the study area.

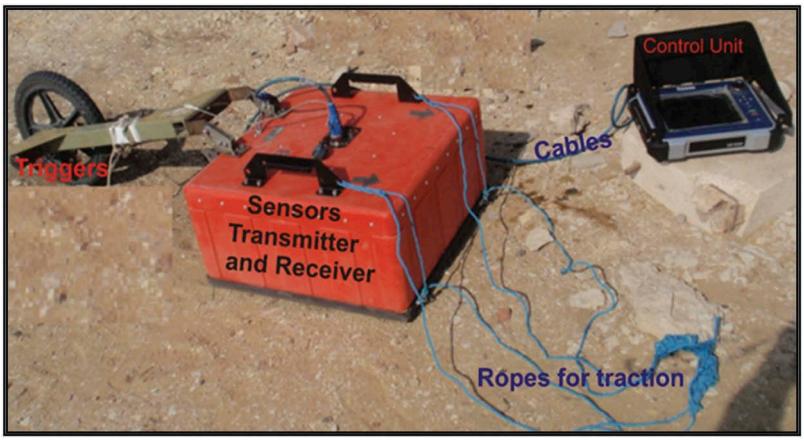

Figure 5. Components of the used GPR system in the study area.

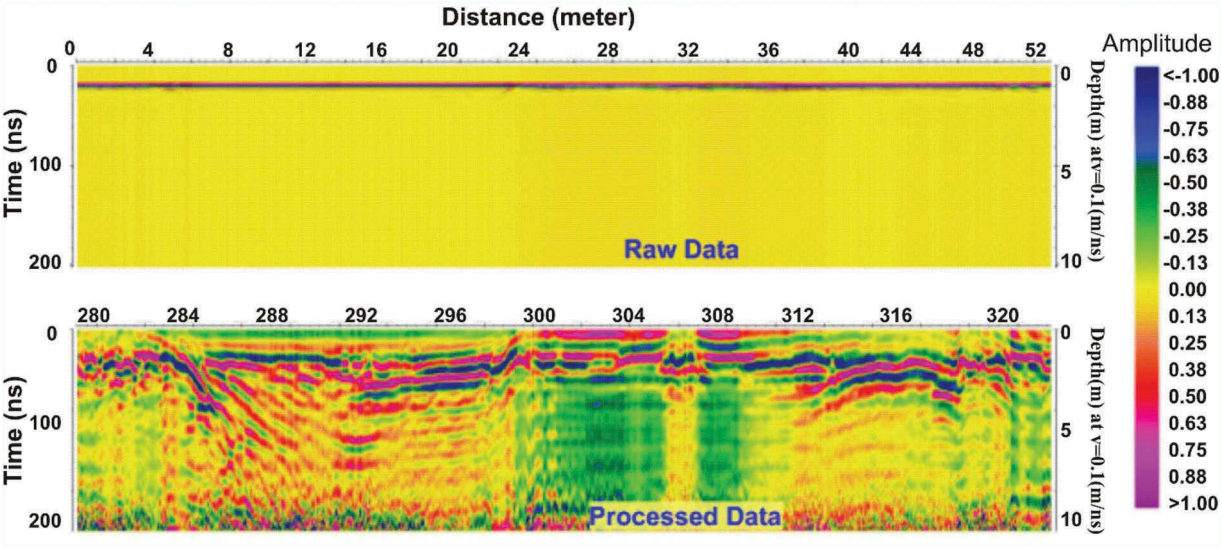

Figure 6. An example of GPR data before and after processing.

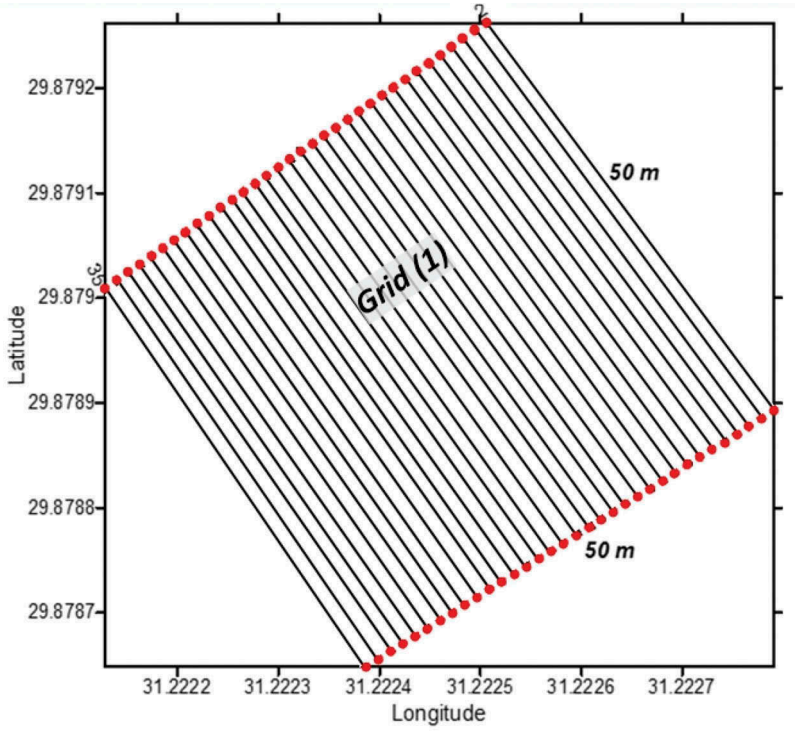

Figure 7. The layout of the GPR profiles for the measured Grid 1.

4. GPR data processing

Data processing is a way to treat the collected data to produce a simple image of the artefact easy to be understood by the classic archaeologists. The present data sets are subjected to processing using the Reflex-Win7 version 8 (Sandmeier 2017). The processing sequences were selected significantly to emphasise the desired signals (signals of use) and depress the undesired signals (noise). These sequences were applied either to individual radar profile separately, or to several sequenced profiles. Simultaneously, the terms and filters within the processing's sequences act either vertically on traces (1D) or horizontally on 2D ranges. Furthermore, the final 2D sections could be arranged to be set in a 3D cubes or intersections. However, in the following, we refer to the most effective processing functions and their physical impact worked over the present data set. Figure 6 shows the GPR record before and after applying the processing sequence as follows:

(1) Subtracting the DC shift; the Transmitter-Ground-Receiver signal pass act similarly as a coupled AC circuit, it generates a phase shift on the received wavefront masking real signal of use. Normally, when the measuring device and processing program of the same brand, it comes automatically to remove the DC shift (phase shift) to retain the zero-mean value. In the present work, the filter acts on each trace (1D) independently, it allows zero mean via subtracting of an existing time constant shift of 5 ns.
(2) Applying a background removing filter to remove the horizontal banding that appears in many GPR records due to the "ringing" of some antennas, horizontal bands are recorded in most profiles (Shih and Doolittle 1984; Sternberg and McGill 1995). These bands can be obscure reflection data that would be visible on some profiles.
(3) Applying a band-pass filter (BPF); this filter is defined by the setting of four frequency values; the first and fourth points determine the low and the high cut frequencies, respectively. The second and third values identify the lower and upper frequency plateau. The relation between the low cut and lower plateau and between the upper plateau and high cut is represented by cosine wave equation. The frequency spectrum values below the low cut and above the high cut frequency are set to zero.
(4) Running average acts on the chosen number of traces. The filter performs running average over a chosen number of traces for each time sample. The filter method suppresses trace dependent

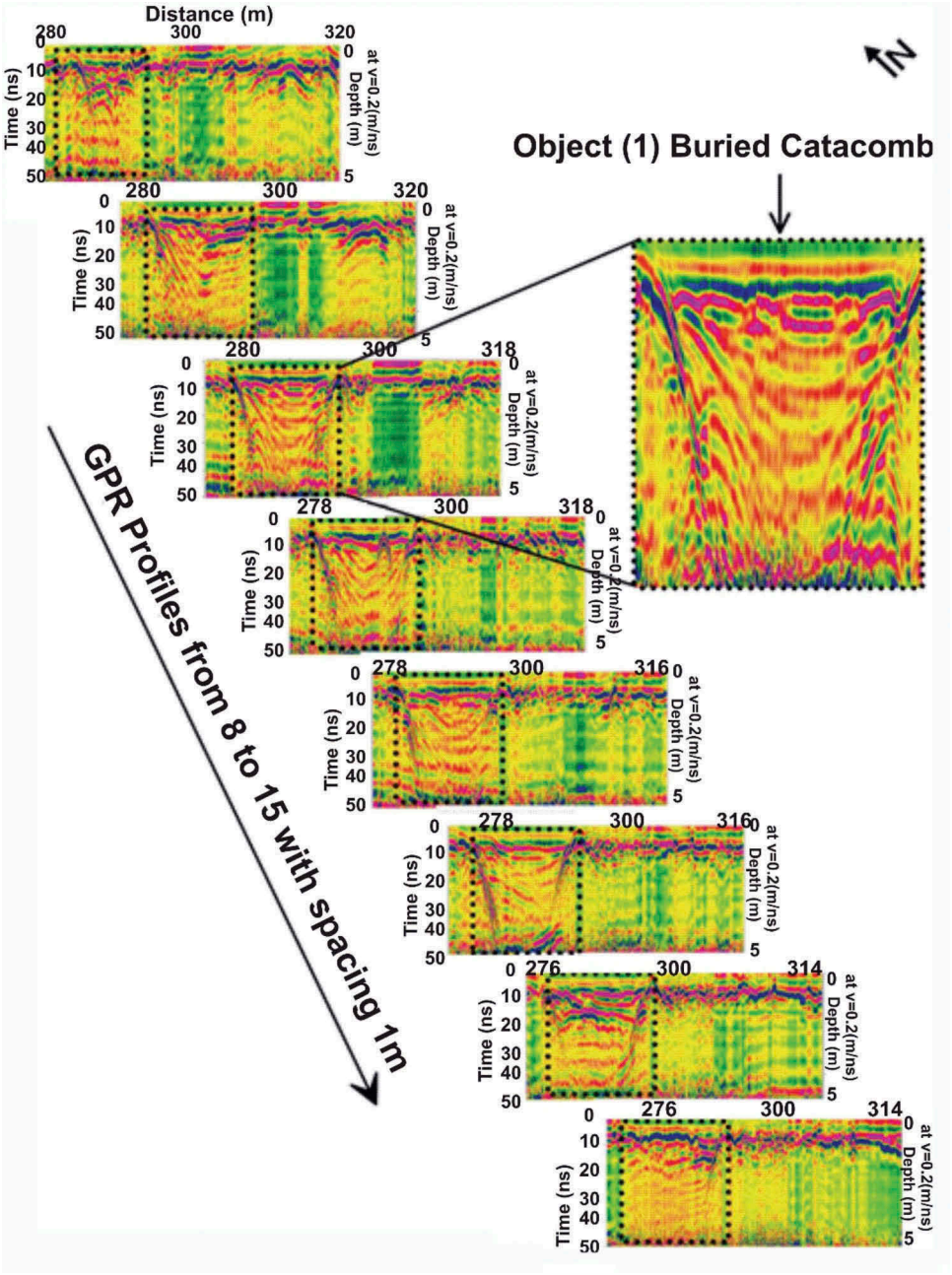

Figure 8. GPR record shows the existence of an artefact, Object (1) could be described as Catacomb.

noise. Its effect is to emphasise horizontally coherent energy.

(5) Employing an energy decay filter: the medium decay curve is specified from the present traces. When the filter is applied on this curve, each datapoint of each trace is multiplied by the decay curve values. When the energy decay curve is multiplied, all data points are multiplied by a decreasing scaling factor.

(6) Constructing a 3D file; this processing step adjusts the data sets to become of similar lengths of the profiles and the number of traces for each via defining the trace increment. The raster of 3D data was based on aligning the 2D profiling (B-Scan) with increment line spacing among all the 2D scans to generate 3D data (C-Scan). When the travel times of the radar pulses are measured, and their intra-ground velocity is known, then distance or depth of the ground can be accurately to eventually render a 3D data set (Shaaban et al. 2009; Conyers and Lucius 1996). The propagation velocity of the radar waves was estimated using the relative dielectric permittivity (RDP) of this area which is represented by hard limestone. According to $\sqrt{RDP} = \frac{C}{V}$, the velocity calculated is 0.100 m/ns. Where c is the velocity of light (0.298 m/ns) and v is the velocity of radar waves.

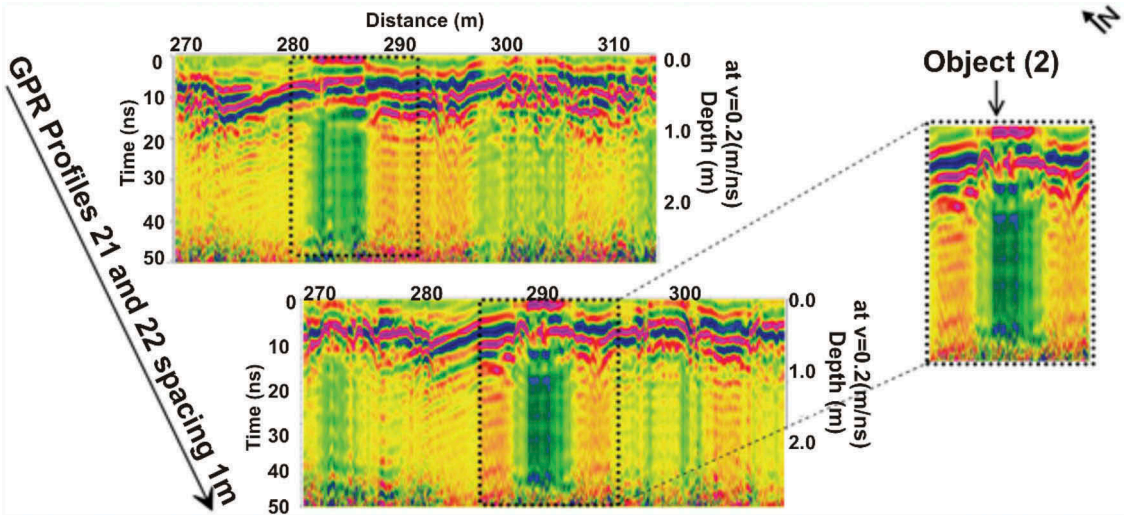

Figure 9. An artefact, Object (2) could be described as carved tomb.

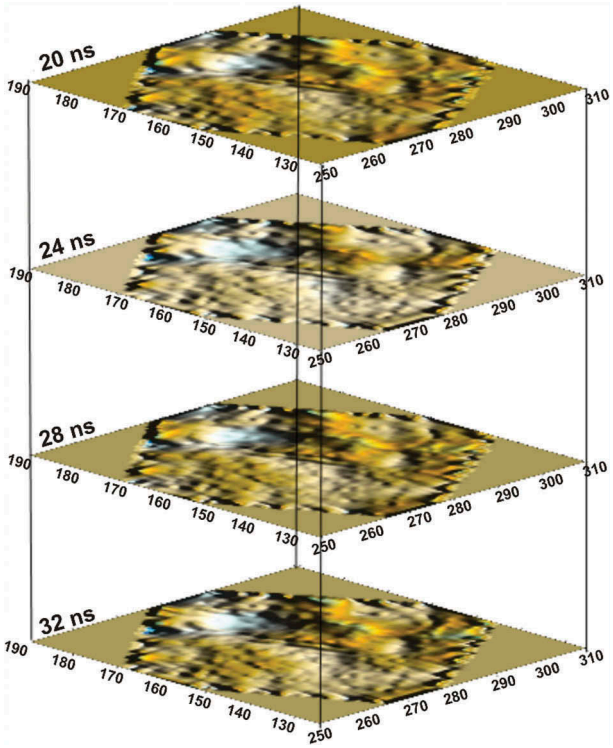

Figure 10. Time slices of Grid 1 at times 20 ns to 32 ns on interval 4 ns.

5. Interpretations

Interpreting the collected data showed the existence of a variety of objects, some of them could be simply identified and others could be estimated according to archaeologist's team knowledge and expertise. In the following, we try to count and describe, as possible, the detectable archaeological objects within each grid and include a correlative map.

5.1. Grid 1

Grid 1 is located in the north-eastern part of the archaeological site of Saqqara area (the animal cemetery) as showing in Figure 3, and it is 50 m in length and 50 m in width. Thirty-four GPR profiles are measured in this grid in the N-S direction as shown in Figure 7. The profile spacing is set as 1.5 m, and the area is completely covered with sand sheet. The results

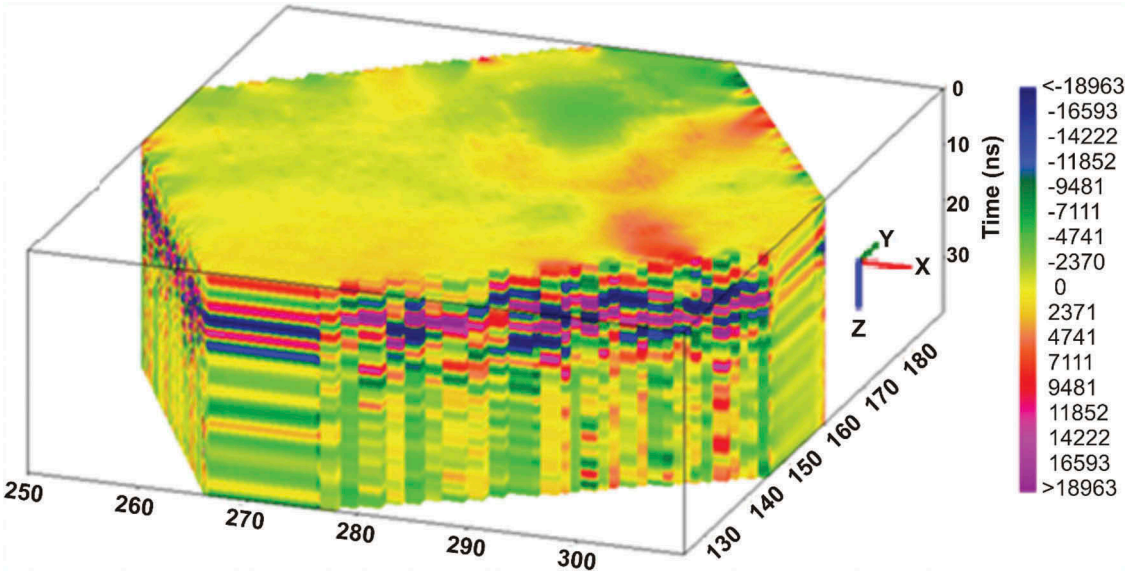

Figure 11. 3D model is showing the extension of the carrying layer of archaeological objects.

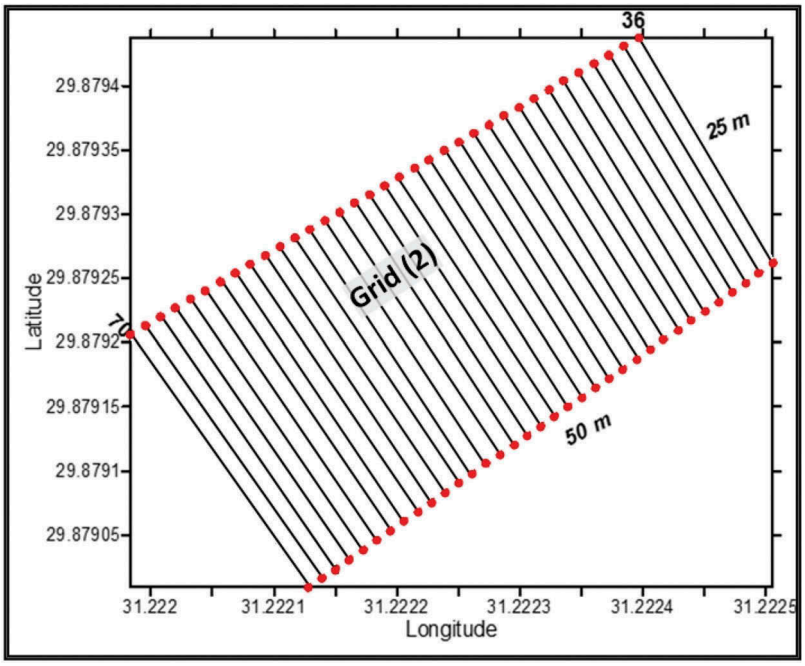

Figure 12. The layout of the GPR profiles for the measured grid.

within this grid demonstrate buried objectives, it seems impossible to count each GPR signature and identify it. Therefore, only few of the clear objects are discussed in the grid. Figure 8 shows an example of the revealed objects, defined as Object (1) herein, extended from line 8 to 15. It is of about 7 m length in the E-W direction, lined with two side walls, and signs of collapse appear in some of its parts. We highly attribute this signature for a catacomb, measurements with the GPR in the perpendicular direction could add other updates for its identity and we plan to conduct an oriented field survey in the near future. A catacomb in our vision, as geophysicists, is a field terminated with two or more sides with buried bodies between them. It is noticed also that the two side walls look sharp from the inner side due to the friable nature of the fill debris as the outer side looks compacted and massive. The catacomb's ceiling and base could be noticed in some place, however, drawing them accurately requires a fine levelling for the ground surface.

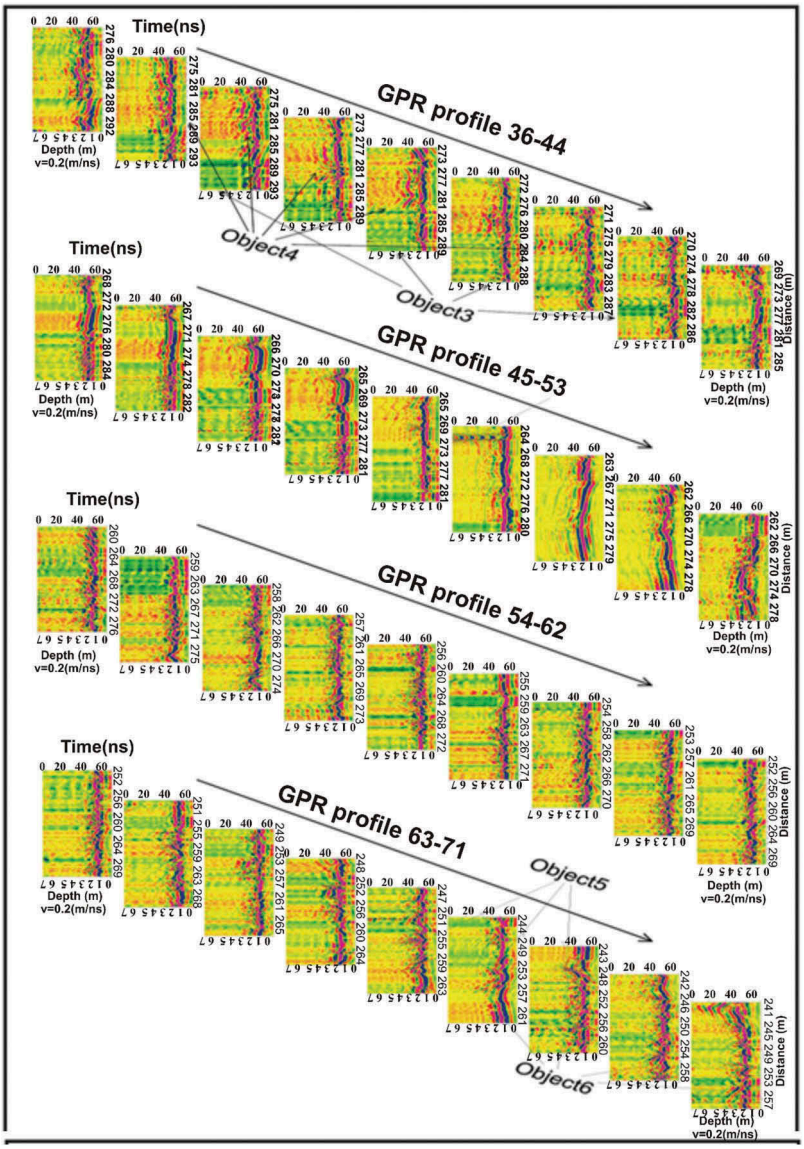

Figure 13. The GPR profiles acquired in Grid 2, the remarkable artefacts are labelled as Object 3, 4, 5 and 6.

We think also that, the north-eastern side wall shows a composite signature, it could be attributed for a second deeper wall, or more likely a coffin of soft material probably wood. Figure 9 shows another object, Object (2) that might refer to a tomb. Our suggestion is based on the nature of its topmost part, which looks like a tomb's cover plate, and it shows a different rock than the tomb's body. We believe also that it is carved in the rock. Figure 10 shows the time slices from 20 ns to 32 ns, it shows the entire Grid 1 with all objects from the generated 3D GPR data of Grid 1 using 1.5 m as profile spacing for the 2D GPR sections.

The profiles show the basic objectives that are evident in the form of anomalies data, which indicates the possibility of the presence of walls or archaeological remains buried. A three-dimensional model (time slicing and 3D cube) showing the extension of the carrying layer of the discovered objects is shown in Figure 11. Time slicing is a technique for creating plan-view maps of an area with specific depth ranges isolated. This not only makes interpretation of the data in the horizontal plane but also allows the user to isolate specific depths for investigation. Time slice technique made the GPR method one of the most precise tools for mapping buried features or objects. Viewing amplitude changes in a series of horizontal time slices within the ground is analogous to studying geological and archaeological changes in equal time-depth layers. The burial features may seem as either low amplitude or high amplitude reflections

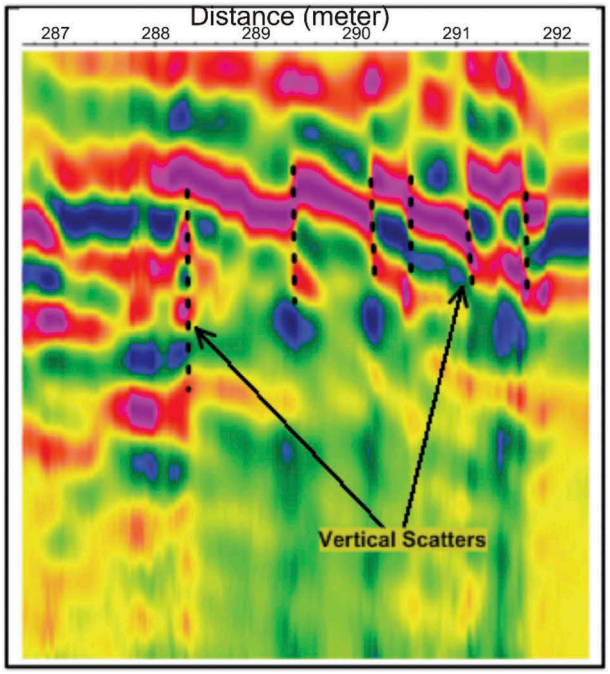

Figure 14. Object 3 from section 37.

in slices, and truncations or breaks in stratigraphy in profiles. Columns and walls seen in profiles as vertically stacked reflections topped with hyperbola. In time slicing maps, walls of the construction will appear as linear reflection, which can be used to define structure extents. Walls and columns generally produce high amplitude reflection due to constructing velocities between walls and surrounding materials.

5.2. Grid 2

Grid 2 (Figure 3) is located adjacent to Grid 1, and it is considered as an extension of Grid 1. It is 50 m length and 25 metres' width. Thirty-five GPR profiles have been measured in this grid in the N-S direction also as shown in Figure 12. Similarly, the profile spacing is set as 1.5 m, and the area is completely covered with sand sheet. A suitable approach is suggested to interpret the 2D GPR record and to consider it the key information for the interpretation instead of the 3D and time slices. The representation of results and GPR response for this grid are found in Figures 13–16. Figure 13 shows the 2D GPR record acquired within Grid 2, the archaeological features are assigned as Object n, where n is the object number.

It is shown from the previous Figures that Object 3 could be seen on several lines. Line 37 is selected to reveal the signature of this object. The width and location of Object 3 on the GPR record vary from place to another. In addition, almost vertical cracks appear and identified as vertical scatters herein. They look stepwise towards the end of the section (as shown in Figure 14). This target is highly recommended for excavation and further investigations.

Figure 15 shows Object 4, which is best seen on line 39, how much it clear is, it is also complicated. It is composed of two adjacent hyperbolas that reflect an object. To the left of the object, it is noticeable an almost similar one of two hyperbolas just wider, where the arrow refers. Moreover, Objects 5 and 6 show impressive signature possible to be interpreted as carved tombs, or at least

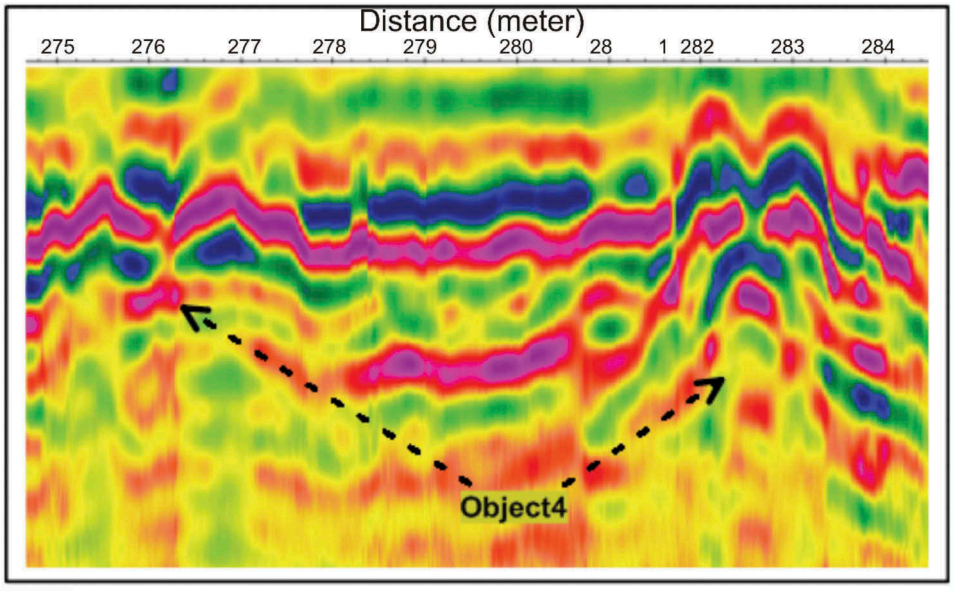

Figure 15. Object 4 from section 39.

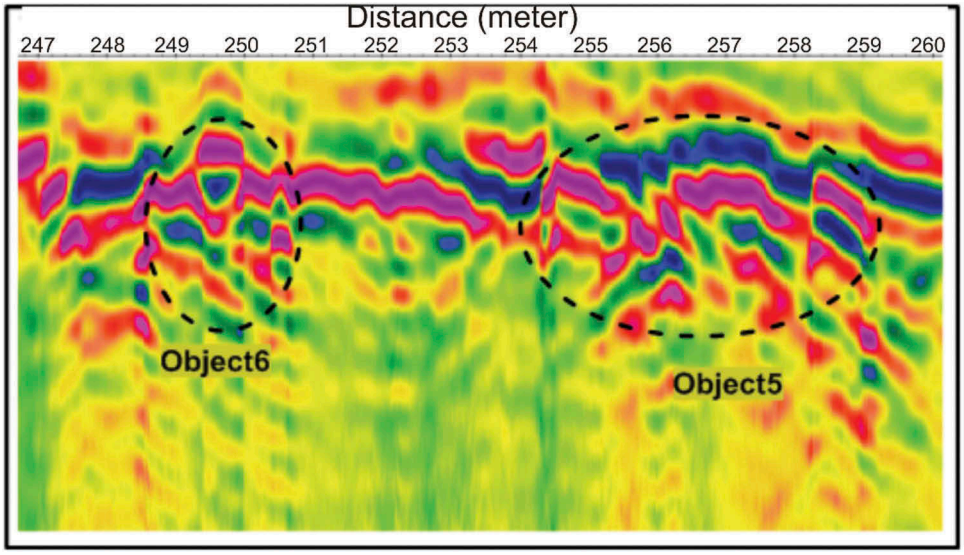

Figure 16. Objects 5 & 6 from section 68.

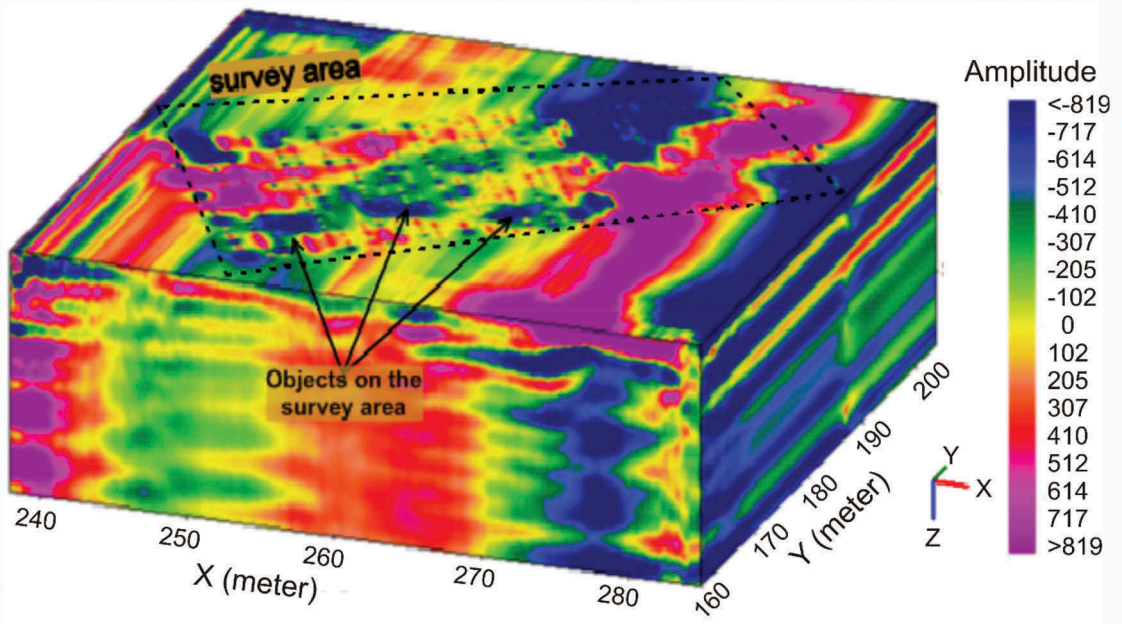

Figure 17. 3D Cube of Grid 2, it shows the survey area, the Z-axis (time) is claimed of the uppermost 15 ns to show the archaeological objects.

significant artefacts (as in Figure 16). Figure 17 depicts a 3D block for the GPR data acquired in Grid 2 where the generated 3D GPR configuration of Grid 2 used 1.5 m as profile spacing for the 2D GPR sections of this grid.

5.3. Free-line grid

The Free-Line grid is located left to Grid 1 and Grid 2. Twelve GPR profiles are measured with a line spacing of 10 m. The profiles length is around 150 m and it is oriented from East to West as shown in Figure 3. A practical field problem is created due to the dimensions of the profile, i.e., length ≈ 150 m, the inter-linear distance10 m with respect to the proposed depth of penetration, and the unevenness of the ground's surface. The illustration of the results is presented in Figure 18, which shows the effect of data compaction at the upper part and dilution at the lower part.

The GPR lines from the Free-Line area are interpreted individually due to the previous reasons; few of the detected features dedicated from the interpretation are

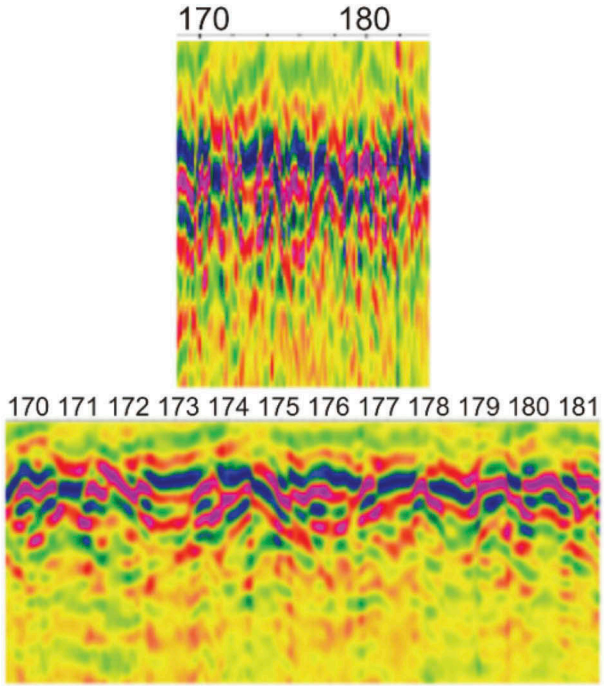

Figure 18. Effect of data compaction on the visualisation quality.

shown in Figure 19. The results imply a recommendation for excavation and further field investigations of the site. Figure 20 shows the tentative interpretation of Grid 1 and Grid 2.

6. Conclusion

The present research was oriented to reveal the potential existence of archaeological artefacts in a site well known for buried artefacts by archaeologists. State-of-the-practice field instrumentations such as SIR4000 connected to a 200 MHz antenna is utilised in this study for subsurface explorations. The site was divided into three grid zones, and field measurements are collected accordingly. GPR data were adequately interpreted as to determine the potential size, shape, depth, and location of the subsurface anomalies that appear on the processed sections, and to discriminate them from the other undesired reflections. The data interpretation tracing the anomalies that appeared on the successive sections to determine the subsurface extend and the

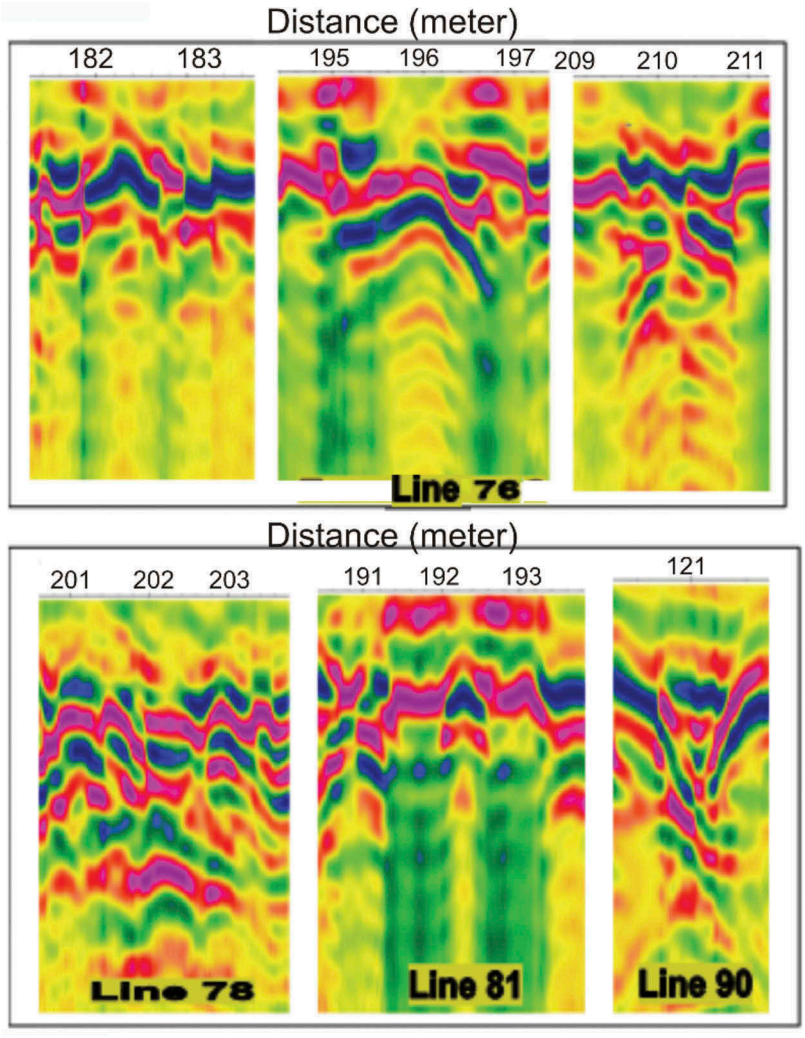

Figure 19. Few GPR signatures from the free-line zone, most of this feature could be an interesting target for excavation.

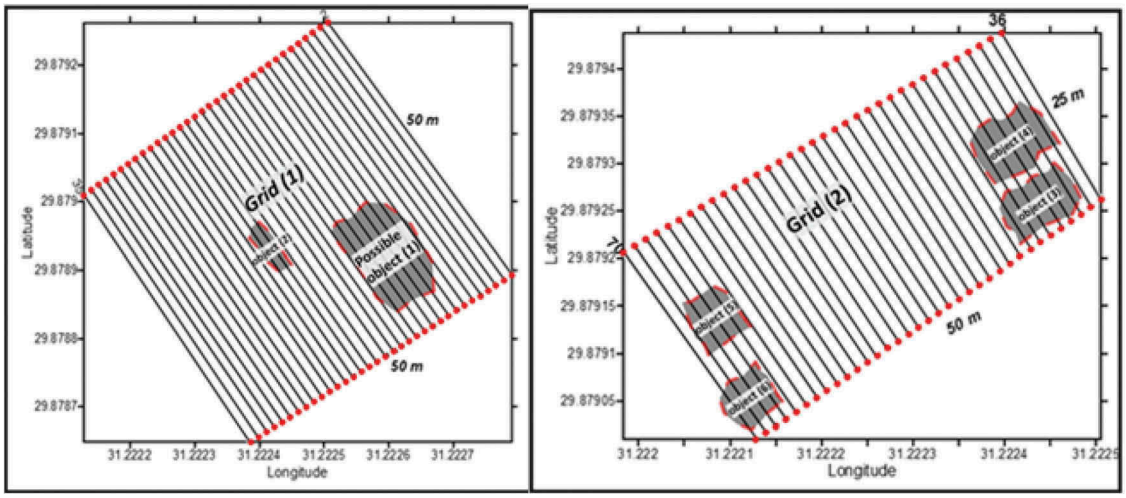

Figure 20. Tentative location of the archaeological objects in Grid 1 and Grid 2.

expected depth of the buried objects that are found in the surveyed three grids. Promising results are drawn with a high probability of artefacts existence underneath the site. Future field investigations and site visits are under preparation to collect more precise data for any future field excavations.

Acknowledgements

This work was performed in the framework of financially supported by the project No.1348. The authors acknowledge the financial support from the Egyptian Academy and Technology for this project. Many thanks also for all individuals and institutions who contribute to the collection of the GPR and GPS data used in this work. The authors greatly appreciate the staff members of the Geoelectric Laboratory, NRIAG, Egypt, for their help in the GPR data acquisition. The authors express their thanks to everybody for valuable discussions and helped for performing this work.

Disclosure statement

No potential conflict of interest was reported by the authors.

ORCID

Nadia AbouAly http://orcid.org/0000-0002-8922-2261
Mohamed Saleh http://orcid.org/0000-0003-3482-7703
Khamis Kabeel http://orcid.org/0000-0002-7134-3954

References

Adès H. 2007. Traveller's History of Egypt. Chastleton Travel: Interlink. ISBN 1-905214-01-4; p. 48.

Atya MA, Shaaban FA, Abbas MA, Hafez MA. 2012. GPR Investigation to the archaeological remains in Mut temple, Luxor, Upper Egypt. NRIAG J Astron Geophys. doi:10.1016/j.nrjag.2012.11.002

Conyers LB, Lucius JE. 1996. Velocity Analysis in Archaeological Ground-Penetrating Radar Studies. Archeological prospection. 3.

Davis JL, Annan AP. 1989. Ground penetrating radar for high resolution mapping of soil and rock stratigraphy. Geophysical Prospecting. 37:531-551. doi: 5 doi:10.1111/gpr.1989.37.issue-5.

Elkarmoty M, Colla C, Gabrielli E, Papeschi P, Bonduà S, Bruno R. 2017. In-situ GPR test for three-dimensional mapping of the dielectric constant in a rock mass. J Appl Geophys. 146:1–15. doi:10.1016/j.jappgeo.2017.08.010.

Hafez MA, Atya MA, Hassan AM, Sato M, Wonik T, El-Kenawy AA. 2008. Shallow geophysical investigations at the Akhmim archaeological site, Suhag, Egypt. Appl Geophys. 5. 136–143.

Hong WT, Kang S, Lee SJ. 2018. Analyses of GPR signals for characterization of ground conditions in urban areas. J Appl Geophys. 152:65–76. doi:10.1016/j.jappgeo.2018.03.005.

Khozym AS. 2003. Geophysical Archaeoprospection in Some Archaeological Sites at El Baharya Oasis, Giza, Egypt: Egypt [Dissertation]. Cairo: Ain Shams University.

Khozym AS. 2007. Geophysical Prospection in some Archaeological sites in Saqqara area, Giza, Egypt: Egypt [master thesis]. Cairo: Ain Shams University.

Lai WWL, Chang RKW, Sham JFC. 2018. A blind test of nondestructive underground void detection by ground penetrating radar (GPR). J Appl Geophys. 149:10–17. doi:10.1016/j.jappgeo.2017.12.010.

Lehner M. 1997. The complete pyramids. New York: Thames and Hudson. ISBN 978-0-500-05084-2; p. 84.

Sandmeier. 2017, https://www.sandmeier-geo.de/.

Sayed H. 2012. Ground Penetrating Radar (GPR) investigations for architectural heritage preservation: the case of Habib Sakakini Palace, Cairo, Egypt. Open J Geol. 2. 189–197.

Shaaban FA, Abbas MA, Atya MA, Hafez MA. 2009. Ground-penetrating radar exploration for ancient monuments at the valley of mummies -Kilo 6, Bahariya Oasis, Egypt. J Appl Geophys. 68(2):194–202. doi:10.1016/j.jappgeo.2008.11.009

Shih SF, Doolittle JA. 1984. Using radar to investigate organic soil thickness in the florida everglades. J Soil Water Conserv.48(3): 651-656. doi: 10.2136/sssaj1984.03615995004800030036x.

Sternberg B, Mcgill J. 1995. Archaeology studies in southern arizona using ground penetrating radar. J appl geophys. 33(1):209–225. doi: 10.1016/0926-9851(95)90042-X.

Trimble NL. 2015. Geomatics software's user manual. Sunnyvale (USA): Trimble Navigation Limited.